ACS APPLIED MATERIALS & INTERFACES

LETTER

www.acsami.org

Graphene-Wrapped Hybrid Spheres of Electrical Conductivity

Sang Ah Ju,[†,‡] Kyunghee Kim,[†] Jung-Hyun Kim,[‡] and Sang-Soo Lee*[,†]

[†]Polymer Hybrid Center, Korea Institute of Science & Technology, Seoul 136-791, Korea

[‡]Department of Chemical and Biomolecular Engineering, Yonsei University, Seoul 120-749, Korea

Supporting Information

ABSTRACT: We present a simple approach for the fabrication of monodisperse electroconductive hybrid spheres using graphene sheet-wrapping via ionic interaction-based self-assembly. The graphene sheets partially charged with anion, which were prepared by controlled chemical reduction of graphite oxide, were mixed with monodisperse polymer nanospheres containing cationic surface charge to form ionic self-assembled hybrid spheres of core−shell structure. The resulting graphene-wrapped hybrid spheres were found to have graphene layer thickness of ca. 10 nm and to exhibit electrical conductivity of 1.33−4.21 S/m as well as monodisperse distributions in shape and diameter.

KEYWORDS: charged graphene, electroconductivity, hybrid spheres, ionic interaction

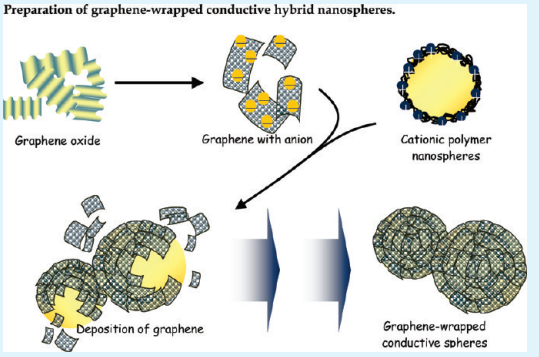

1. INTRODUCTION

In recent years, composite particles consisted of host and guest materials of nanometer to micrometer length scales have drawn much attention because of the interesting properties derived from their hybrid structure.[1−3] Especially, metal−polymer composite particles of electrical conductivity can play an important role in diverse fields such as optics, electronics, catalysis, and biotechnology.[4−8] The large attention on developing novel strategies for metal-based composite particles reflects the extremely high demand of key technologies, such as microelectronics. These metal-based conducting composite particles have been extensively researched as a key element, especially in microelectronic packaging materials such as anisotropic conductive adhesives (ACAs). Recently, conductive particle−embedded composite materials are becoming popular as a promising candidate for lead-free interconnection solution in microelectronic packaging applications due to their technical advantages such as fine pitch capability (<40 μm pitch), low temperature processability, low cost, and so on.[9−14] Many kinds of conductive composite particles have been fabricated through self-assembly mechanism, which promise to provide a facile and versatile pathway to the assembly of small particles, and to control the functionality in such colloidal systems.

The most successfully commercialized example of functional composite particle is the metal-coated polymer microspheres, of which core polymer spheres are usually decorated with metallic component to provide electrical conductivity.[15−18] However, poor interfacial adhesion between two incompatible materials, metal and organic polymer, causes severe delamination of metallic layer from the surface of polymer spheres as well as formation of voids, and this has been a critical issue in aspects of the performance, stability and durability of conductive particles, especially when applied for the microelectronic connection. To improve the interfacial compatibility, an additional layer capable of providing covalent bonding between metallic shell and polymer core has been introduced on the conductive ball, and results in the enhancement of interfacial stability between the conductive ball and polymer matrix up to a certain point was reported; however, it is not enough to ensure the reliability and durability of conductive particles without loss of electric conductivity. Furthermore, most of the incorporation methods of metallic components to host polymer ball including metal-plating or surface seeding methods have been inevitably required to use highly toxic chemicals possibly causing a serious environmental issue.

As is well-known, graphene, two-dimensional graphitic nanosheet, exhibits remarkable electronic properties that quantify it for applications in future cutting-edge devices. To date, most of the research concerning the applications of graphene have been poured into the evaluation of natural properties of graphene itself,[19−23] mass production of well-crystalline graphene nanosheets[24−26] or nanocomposite applications,[27−30] such as transparent conductive films via simple mixing of graphene with matrix materials. Although they are good candidates for structural, electrical and thermal applications, the potential applications of graphene nanosheets are hindered by the tedious exfoliation process of bulk graphite and the manipulation difficulties owing to their insolubility and poor dispersion in common organic solvents or polymeric matrices. Recently, our group found that the fabrication of three-dimensional functional materials from two-dimensional graphene nanosheet, such as electrically conductive micro/nanoparticles is a highly efficient method to provide application of graphene with retention of the intrinsic electrical conductivity.

Received: January 16, 2011
Accepted: March 23, 2011
Published: March 24, 2011

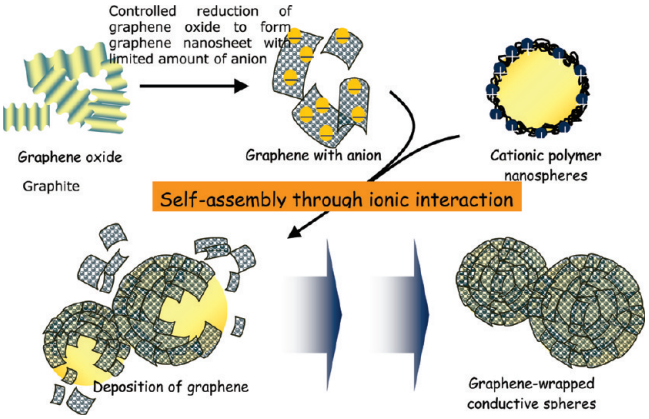

Figure 1. Schematic illustration of preparation of graphene-wrapped conductive hybrid nanospheres.

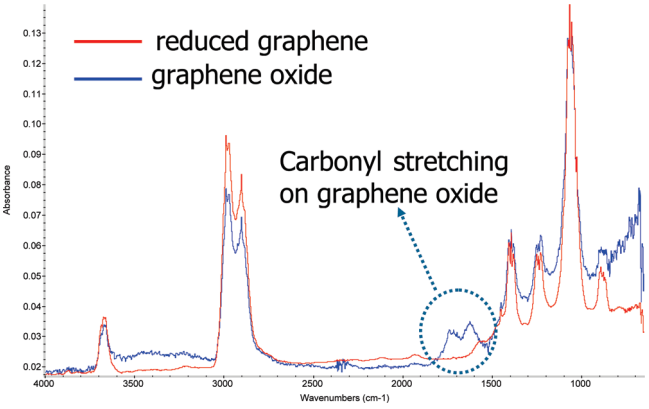

Figure 2. FT-IR spectra of graphene oxide and graphene after chemical reduction.

Recently, several studies have demonstrated that single or multiwalled carbon nanotubes can be assembled onto the surface of colloidal spheres, and Vickery et al. showed that graphene-coated polymer spheres can be prepared via ionic interaction.[31−33] In most cases, however, a large amount of charge formation on graphene sheet, which is demanded to complete ionic interaction was given through extensive chemical oxidation of graphite and coating of graphene sheet with charge donating molecules such as polystyrene sulfonate, resulting in inevitable loss of conductive nature. Herein, we present a novel and extremely simple approach for the fabrication of graphene-wrapped polymer nanospheres with electrical conductivity.

2. EXPERIMENTAL METHODS

Materials. Styrene (Aldrich) was purified by passing them through an inhibitor removal column. (2-methacryloyloxy) ethyl) trimethyl ammonium chloride (MATMAC, 75 wt % aq. solution, Sigma-Aldrich), calcium stearate (Aldrich), potassium persulfate (KPS, Aldrich), sulfuric acid (95−97%, Aldrich), hydrogen peroxide (Aldrich), hydrazine monohydrate (35% in water, Aldrich), and ammonia solution (28 wt % in water, Junsei) were used as received.

Preparation of Anion-Charged Graphene Sheets. Negatively charged graphene sheets were prepared through chemical oxidation of expandable graphite flake (Graftech) using a modified Hummer's method, followed by reduction using hydrazine hydrate as noted in refs 37 and 41. First of all, the ground graphite flake

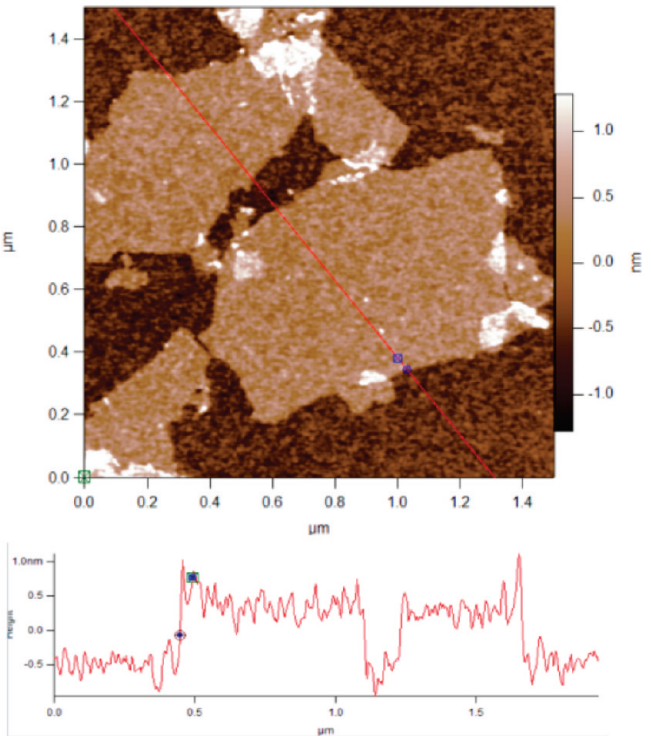

Figure 3. Tapping-mode AFM image of graphene nanosheets after reduction of graphene oxide with a cross-sectional height profile taken along the red straight line. The sample was prepared by drop-casting dilute graphene dispersion onto a silicon wafer.

(~0.85 g) was stirred in 98% H_2SO_4 (23 mL) for 8 h, and $KMnO_4$ (3 g) was gradually added to the dispersion while keeping the temperature below 20 °C. Next, the mixture was diluted with distilled water and heated at 100 °C for 30 min. The reaction was terminated by addition of distilled water (140 mL) and 30% H_2O_2 solution (10 mL). The mixture was washed by repeated centrifugation at 8000 rpm for 30 min, first with 5% HCl aqueous solution, and then distilled water. The resulted graphite oxide was suspended in water to give a brown-colored dispersion, which was subjected to dialysis to completely remove residual salts and acids.

Exfoliation of the obtained graphite oxide to graphene oxide (GO) was achieved by ultrasonication of the dispersion using a Hielscher Ultrasonics (UIP 1000hd, 150W, 50% amplitude) for 30 min. The obtained brown dispersion was then subjected to 30 min of centrifugation at 3000 rpm to remove any unexfoliated graphite oxide (usually present in a very small amount).

Finally to obtain negatively charged graphene sheets, homogeneous dispersion (100 mL) of the synthesized graphene oxide was mixed with 250 mL of distilled water, 10 mL of hydrazine solution and 700 μL of ammonia solution in a 500 mL round bottomed flask. The weight ratio of hydrazine to GO was about 70:1. Under intensive stirring, the dispersion was put in a oil bath controlled at 95 °C for 1 h. Excess hydrazine in the resulting dispersion was extensively removed by repeated dialysis against ammonia solution once the reduction is complete. The obtained dark grayed dispersion was then subjected to centrifugation of 1 h at 10 000 to 50 000 rpm, coupled with ultrasonication for 30 min to control lateral length of the sheets.

Preparation of Cation-Charged Polymer Beads. Positively charged polystyrene beads of two different sizes (cationic microsphere and nanosphere) were prepared by emulsifier-free emulsion

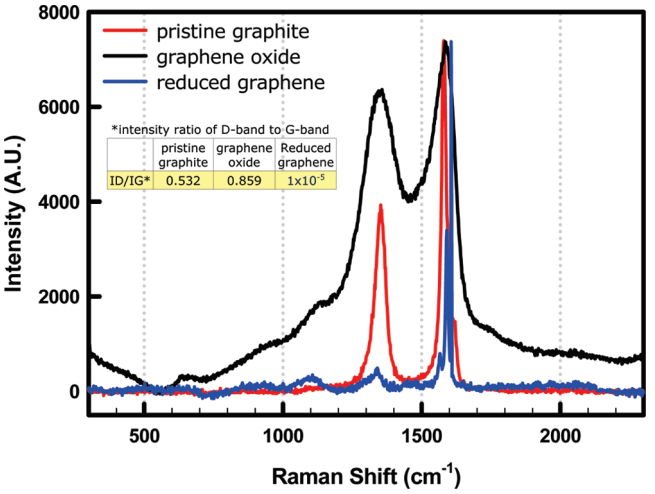

Figure 4. FT-Raman spectra of pristine graphite, graphene oxide, and graphene after chemical reduction.

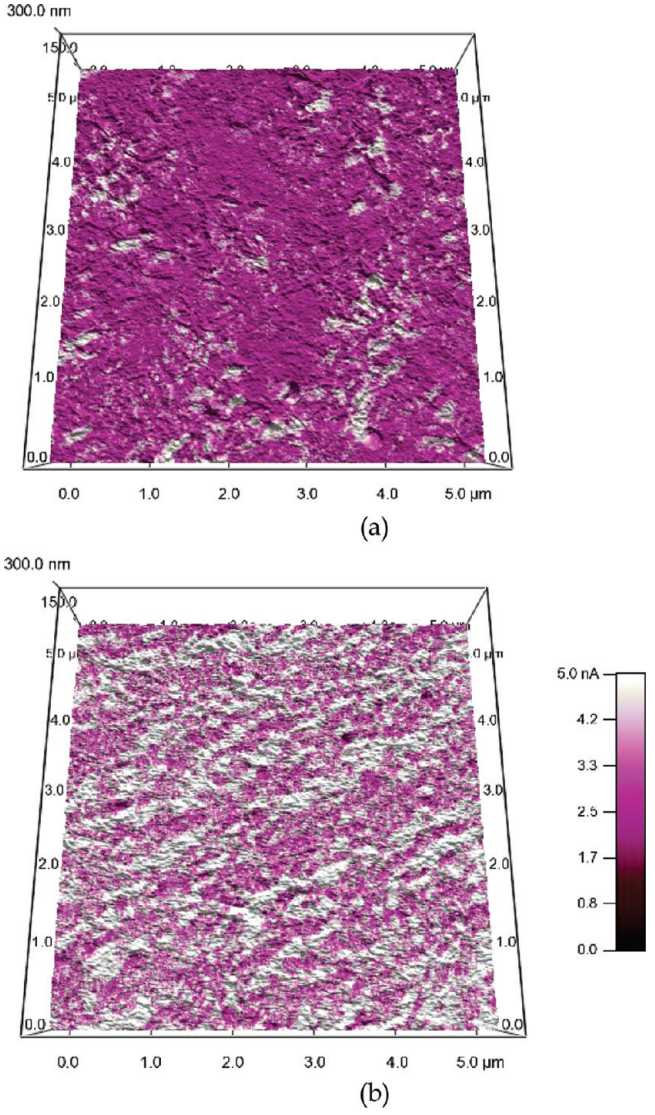

Figure 5. Conducting-mode AFM images of (a) graphene oxide and (b) graphene sheets. The gray-colored area denotes electron transporting pathway.

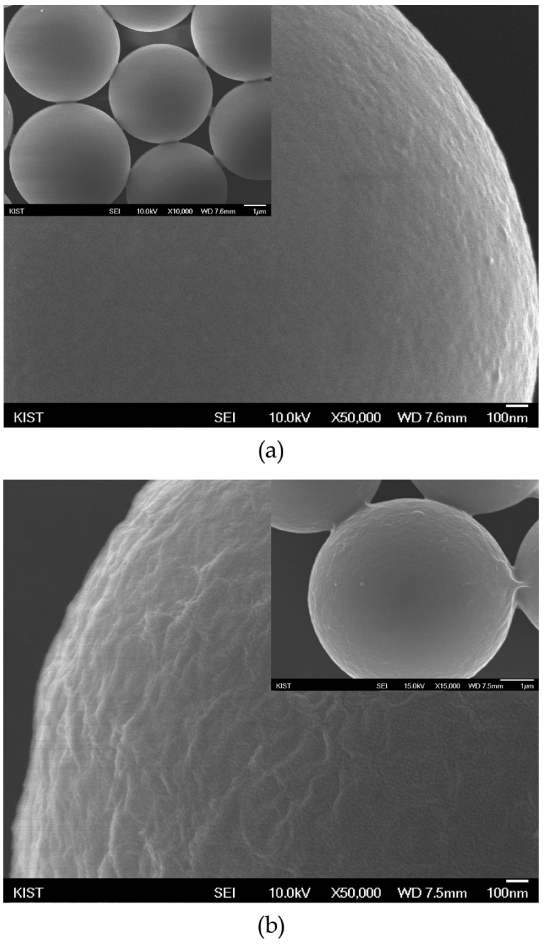

Figure 6. Scanning electron microphotographs of spheres of 5 μm diameter (a) before mixing with graphene and (b) after mixing with graphene.

copolymerization. To obtain microsized positively charged PS spheres, we at first added 200 mL of deionized water to the reactor, followed by deoxygenating by extensive bubbling with nitrogen for 30 min. The mixture of styrene (10.42 g, 0.1 mol) and MATMAC (0.05 mol) were added into the reactor, followed by addition of 0.1 g of KPS dissolved in 10 mL of deionized water. The polymerization was carried out under mechanical stirring at 400 rpm under a nitrogen atmosphere at 70 °C for 8 h. Products were purified through dialysis using cellulose tubular membrane (membrane filtration products) for 7 days.

To obtain nanosized positively charged PS spheres, mixture of calcium stearate (0.5 mM) and 20 g of styrene monomer (0.96 M) was added to 200 mL of 1N-NaOH aqueous solution with moderate stirring, resulting in milky emulsion. The polymerization of styrene monomers including calcium stearate was initiated by addition of 0.73 mM aqueous solution of KPS at 70 °C under nitrogen atmosphere. The polymerization reaction was carried out for 6 h and terminated by quenching to 0 °C. The synthesized colloidal nanospheres were washed several times with methanol and then with water during extensive centrifugation cycles. Products were purified through dialysis using cellulose tubular membrane (membrane filtration products) for 7 days.

Assembly of Cationic PS Spheres with Anionic Graphene. Positively charged PS spheres (0.08 g) and negatively charged graphene sheets (0.05 g), respectively dispersed in deionized water, were mixed on sonicator for 30 min and then were

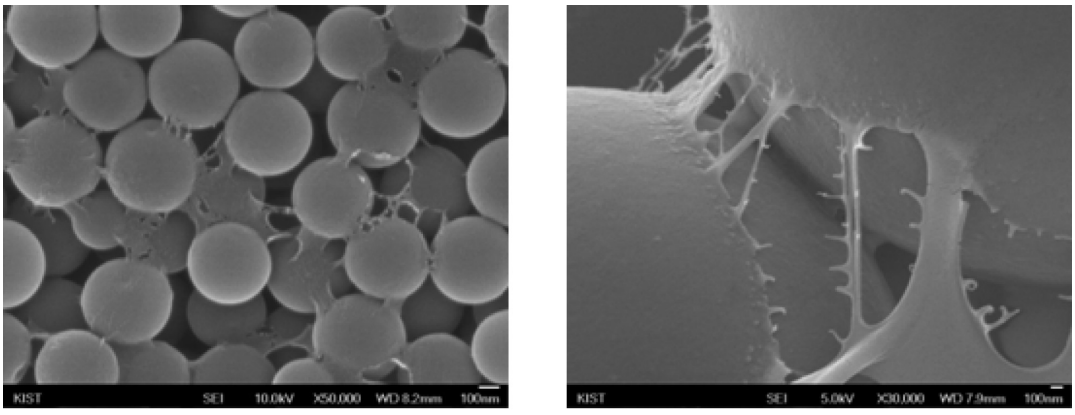

(a)

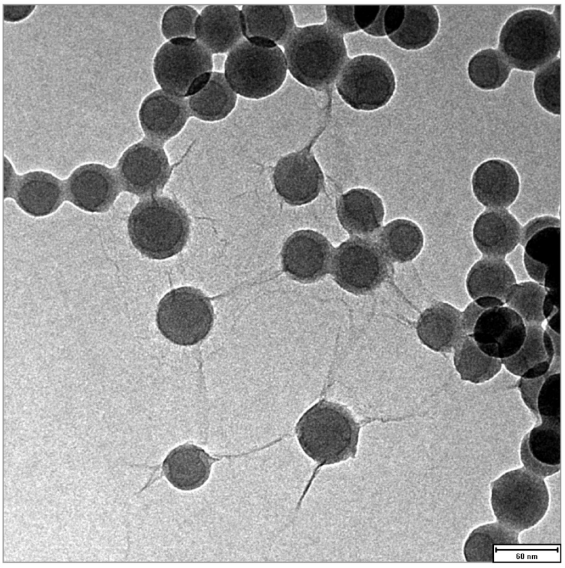

(b)

Figure 7. (a) Scanning electron microphotographs and (b) transmission electron microphotograph of graphene-wrapped hybrid spheres.

vigorously shaken for 12 h at room temperature on vortex shaker (Maxi Mix II, Fisher). Subsequently, the coagulates were collected by centrifugation of 5000 rpm and dispersion in water at least three times, and finally dried on freeze-dryer for 24 h.

Characterization. The size and size distribution of cationic PS spheres and hybrid spheres, respectively, were determined by dynamic light scattering (ELS-8000, Otsuka Electronics). Zeta potentials of graphene and cationic PS spheres were determined using a laser electrophoresis zeta potential analyzer (Zetasizer 3000HSA, Malvern Instruments). The analyses were carried out at 25 °C and the zeta potential was taken as the average of five measurements. The morphology of cationic PS spheres and hybrid spheres was characterized by field emission-scanning electron microscope (JSM-6701F, JEOL) working on accelerating voltages of 5 to 15 kV. The specimens were platinum-coated prior to examination. TEM images were acquired using a JEOL 3000F transmission electron microscope. The accelerating voltage was 300 kV. One drop of graphene-wrapped hybrid spheres/water suspension (or neat graphene/water suspension) was placed on a carbon coated Formvar grid. Samples were used after drying at room temperature for overnight. Atomic force microscopy (AFM) imaging was performed on Nanoscope III (Asylum). AFM images were obtained in tapping mode with RTESP model Si/N tips and conductive mode. 1 cm x 1 cm silicon wafers used for spin coating of the solution were soaked in Piranha solution for 1 h, followed by thorough rinsing with distilled water and drying under nitrogen atmosphere. A small drop of graphene-wrapped hybrid spheres/water suspension (or neat graphene/water suspension) was placed on the prepared substrate and spin-coated at 2000 rpm for 30 s, followed by AFM investigation.

FT-Raman spectroscopy was performed on RFS-100/s (Bruker) using 1064 nm incident laser wavelength. The incident laser power was carefully tuned to avoid sample damage or laser induced heating and measurements were thus performed with an incident laser of power density of about 0.5 mW/cm^2.

Electrical conductivity measurement was performed using the four-probe method to eliminate the effect of contact resistance. A Keithley 6512 digital multimeter equipped with a YEW 2553DC voltage current standard was used to measure the $I-V$ characteristics of the samples at room temperature.

3. RESULTS AND DISCUSSION

In Figure 1, the preparation procedure of graphene-wrapped polymer nanospheres is illustrated; the solution-based chemical

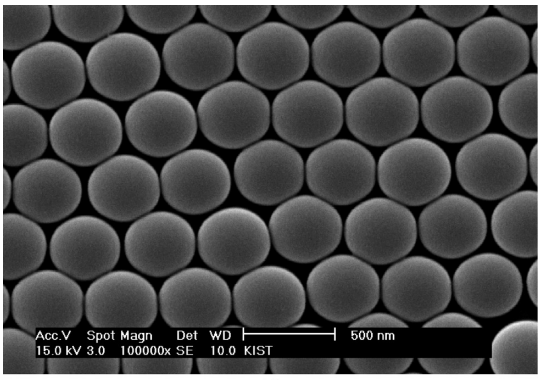

(a)

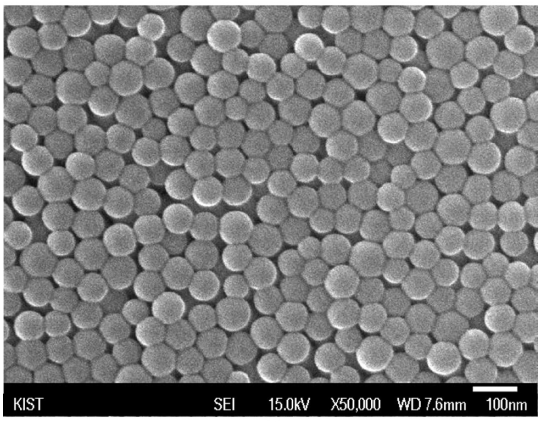

(b)

Figure 8. Scanning electron microphotographs of graphene-wrapped hybrid spheres of (a) 400 and (b) 80 nm diameter, which were prepared using lateral length-controlled graphene sheets.

oxidation of graphite easily generates hydrophilic graphite oxide, which can be readily exfoliated as individual graphene oxide (GO) sheets by ultrasonication in water.[34,35] GO can be converted back to graphene by chemical reduction, for example, using hydrazine. As recently demonstrated,[36,37] the formation of stable GO colloids is largely attributed to electrostatic repulsion as a result of ionization of the carboxylic acid and phenolic hydroxyl groups that are known to exist on the GO sheets, rather than just the hydrophilicity of GO. If carboxylic acid groups are not perfectly reduced by hydrazine under the given reaction condition, these groups should therefore remain in the reduced product. During suspending in water medium, the negatively charged graphene sheets are mixed with colloidal polymer spheres containing cations, and the attractive force between anion and cation should result in graphene-wrapped hybrid spheres.

Before assembling hydrazine-reduced graphene sheets with cationic polymer spheres, colloidal GO and reduced graphene sheets were analyzed by FT-IR as shown in Figure 2. There was no notable change in the absorption peak of 3700 cm^{-1}, which is related to free phenolic hydroxyl group dangled on GO and partly reduced graphene surface. On the other hand, a very broad absorption band around 3000−3500 cm^{-1} regime for GO, which is related to the presence of carboxylic acid, was highly suppressed for the reduced graphene. Furthermore, the intense carbonyl peaks of 1740 and 1630 cm^{-1}, which are respectively related to the presence of carboxylic acid and ketone, were hardly detected for the reduced graphene, implying that hydrazine-based reduction reaction of GO was successfully performed. However, as expected, graphene sheets also showed the partly survival of polar groups including carboxylate anion and hydroxyl groups at around 1550 and 3700 cm^{-1},[38] suggesting that the surface of the graphene sheets in aqueous solution should still be charged after reduction. The feasibility of forming anion-charged graphene sheets is further supported by zeta potential measurement. The GO obtained from chemical exfoliation of graphite showed a zeta potential of −42.79 mV, supporting its high dispersion stability in water medium, and the graphene obtained from hydrazine-based reduction of the former GO showed −36.01 mV, implying that the anionic charge, although the amount was reduced due to the recovery of graphitic sp^2 structure from sp^3, is partly reserved even after reduction.

The graphene sheets recovered from colloidal GO were also examined by AFM under tapping mode, which shows that the products obtained from hydrazine-based reduction of the GO that are cast on a silicon wafer were flat, with a thickness of ∼1 nm as given in Figure 3, implying that exfoliation from graphite to graphene sheets was perfectly accomplished as intended.

One major drawback of the chemical exfoliation of bulk graphite to graphene nanosheet by chemical method via GO is possible formation of various defects such as destruction of hexagonal structure employing carbon atoms of sp^2 orbital; the electronic properties of the graphitic structure are possibly deteriorated by destruction of the intrinsic chemical structure. In this work, we need the formation of anionic graphene sheets without large loss of the intrinsic electrical nature during chemical treatment, and thus, monitoring of formation of defects during graphene preparation using FT-Raman has been tried. FT-Raman spectra for graphite flake, GO and graphene sheets show two major peaks in the high frequency range; the tangential mode or so-called G-band at 1580 cm^{-1} corresponding to the first-order scattering of the E2g mode and D-band at 1340 cm^{-1} assigned to carbonaceous compounds or defects in graphitic carbons.[39−41] As found in the case of carbon nanotube, intensity ratio of D-band to G-band can be a useful indicator telling the change of relative concentration of defect of graphitic carbon structure. As shown in Figure 4, the intensity ratio of D-band to G-band increased during oxidative exfoliation from pristine graphite to GO, followed by huge drop of intensity ratio during reduction from GO to graphene, suggesting that the sp^2 graphitic carbon structure within the graphene sheets is highly restored upon reduction by hydrazine.

As is well-known, exfoliated GO is electrically insulating. Therefore, at least partial reduction of GO would be required to restore electrical conductivity. To find an evidence supporting FT-Raman result, AFM examination under conductive mode with a bias voltage of 100 mV has been performed; while the specimen of GO spin-coated on silicone wafer does not show any evidence of conductivity (Figure 5a), the specimen of graphene reduced from GO exhibited well development of bright-colored network showing electron transporting pathway (Figure 5b), implying that the chemical reduction to graphene from GO was successful.

To obtain hybrid spheres of electrical conductivity, assembly of graphene sheets containing anion charge with cationic polymer spheres (micro and nanospheres, respectively) was performed by simply mixing them together in deionized water medium. We found a spontaneous change of dispersion from respective colloidal states of graphene and polymer spheres to irreversible agglomerates, indicating the formation of graphene-polymer sphere assembly accompanied by spontaneous anion−cation coupling reaction.

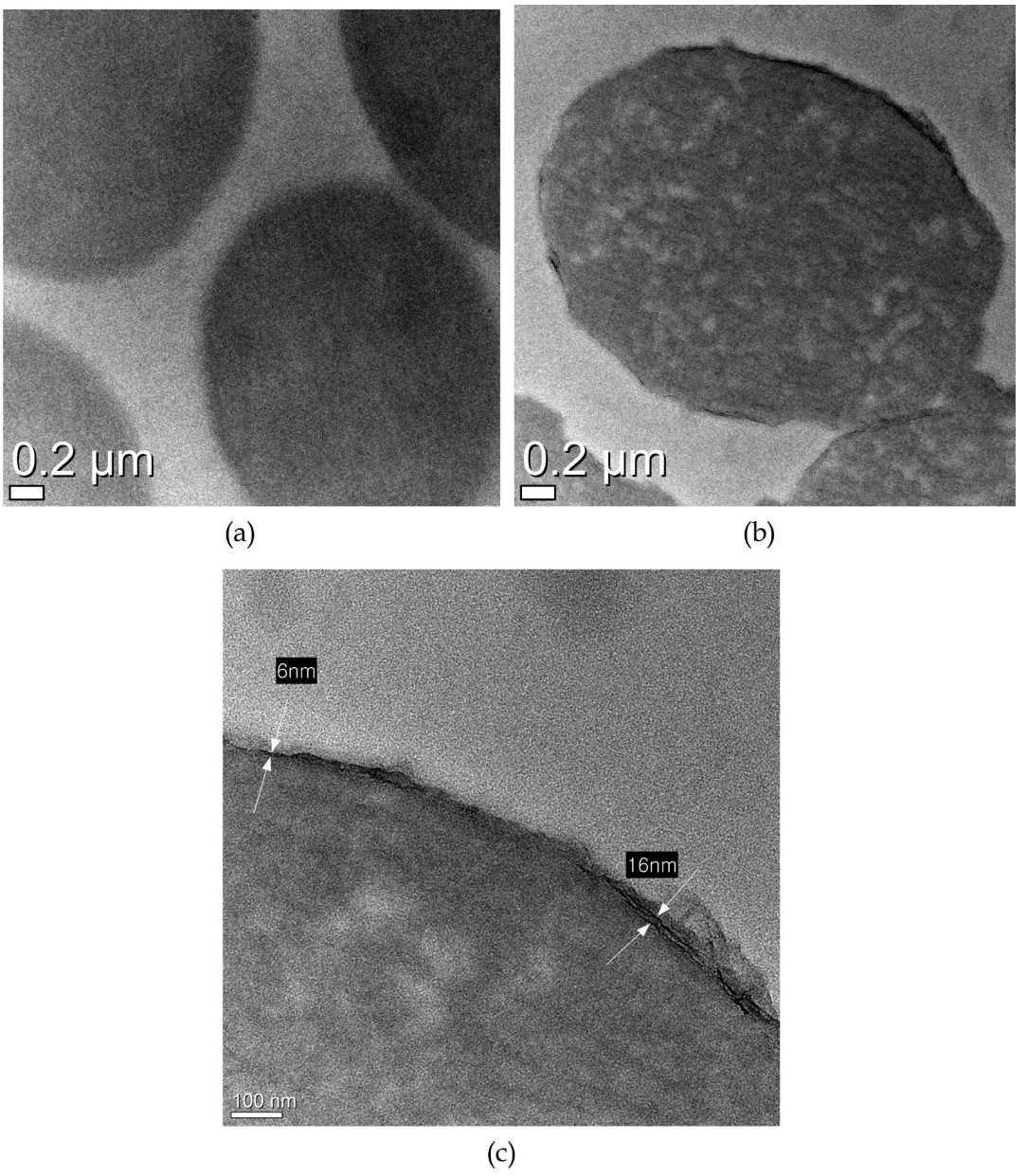

Figure 9. Transmission electron microphotographs of (a) pristine host polymer microspheres, (b) graphene-wrapped hybrid microspheres, and (c) the zoom-up image of hybrid microsphere showing highly thin graphene layer adsorbed on polymer sphere.

Table 1. Electrical Conductivity for Spray-Coated Glass Cell by Four-Probe Method

material spray-coated on glass cell	electrical conductivity (S/m)
pristine graphite	15.5
reduced graphene nanosheets	10.7
graphene-wrapped hybrid spheres (5 μm diameter)	1.33
graphene-wrapped hybrid spheres (400 nm diameter)	4.21

Electron microscopic examination was performed to analyze the assembly behavior between polymer spheres and graphene sheets. In Figure 6, SEM images obviously show that the polymer spheres were successfully decorated by graphene nanosheet patch. While the pristine colloidal polymer spheres in Figure 6a do not exhibit any notable feature except smooth surface, the surface of polymer spheres after assembly with graphene sheets showed very rough texture, as shown in Figure 6b, implying that there are adsorbed layer of texturing molecules on polymer spheres.

When reducing the diameter of cationic polymer spheres from 5 μm to 600 nm, graphene sheet could adhere on one more polymer spheres rather than wrapping each sphere, resulting in

ligament formation among spheres, as shown in Figure 7a. Furthermore, as the diameter of cationic polymer spheres decreased further to 80 nm, thin fibrous structures propagating away from the hybrid spheres as well as bridges linking neighboring spheres were also formed, as shown in Figure 7b. Because fresh graphene recovered from chemical treatment of bulk graphite exhibits broad size distribution, the assembly of polymer spheres with just-reduced graphene resulted in that some portion of hybrid spheres was tethered by graphene sheet, as shown in Figure 7. The tethering of hybrid spheres or ligament formation by graphene were found to become prevailing as the diameter of host spheres decreased. A sheet of graphene, if appropriately large, possibly adheres to one more spheres simultaneously. To suppress the formation of graphene bridge linking neighboring spheres and to obtain discrete hybrid spheres, it is demanded that the lateral length of graphene sheet should be tailored not larger than the diameter of polymer spheres to be wrapped by graphene. For that purpose, lateral length selection of graphene sheets using ultracentrifugation coupled with high power ultrasonication was performed with monitoring on dynamic light scattering (refer to Figure S1 in the Supporting Information), and graphene sheets with nominal lateral length below 200 nm were collected for assembly. As shown in Figure 8, the result was successful; all the hybrid spheres were collected without any evidence of aggregation or bridging induced by graphene sheets regardless of the diameter of host spheres.

In this system, the ionic interaction drove the graphene sheet to anchor on the polymer surface. Although the repulsive force among anionic graphene sheets should suppress the formation of multilayered adsorption of graphene on the surface of cationic polymer spheres, it was found that deposition of anionic graphene sheets on the cationic surface of polymer spheres seems to occur rapidly to form graphene-polymer hybrid spheres without any void surface. Deposition of graphene sheets on polymer sphere is supported by transmission electron microscopy examination in Figure 9, showing that thin layer of graphene sheet was well-deposited on the surface of polymer spheres to thickness of 5−16 nm.

To assess the electrical conductivity of graphene-wrapped hybrid spheres, we respectively prepared the suspension of pristine graphite, reduced graphene, and graphene-wrapped hybrid spheres of different diameter (5 μm and 400 nm) in ethanol medium, and sprayed them on a fresh slide glass heated at 150 °C to form a conductivity measurement cell, which was then tested under four-probe method. As found in Table 1, although pristine graphite showed electrical conductivity of 15.5 S/m, the conductivity of reduced graphene nanosheets was lowered to 10.7 S/m, implying imperfect reduction of GO to graphene with defects as revealed in FT-Raman and FT-IR results. On the other hand, the hybrid spheres of 5 μm diameter exhibited an electrical conductivity of 1.33 S/m, and decrease of diameter of the spheres to 400 nm induced an increase of conductivity to 4.21 S/m, proving the number of ohmic contact would be critical factor determining electrical conductivity. The somewhat lower electrical conductivity of the cells made with graphene-wrapped hybrid spheres might be possibly due to the partial lack of ohmic contact in the cell as well as the electronic interfacial change. Nevertheless, it can be told that the electron transfer behavior found in graphene sheets is preserved even after the formation of hybrid with insulating polymer spheres. We believe there is room for improvement, such as increasing conductivity of graphene-wrapped hybrid via the use of graphene sheets of better electrical conductivity tunable by chemical preparation condition as well as the new geometry of assembly.

It should be noted that the concept of using graphene-wrapped hybrid spheres as conductive medium works well, even in a nonoptimized state. The advantages of our approach include cheap and abundant carbon resources and simple fabrication procedures.

■ ASSOCIATED CONTENT

Ⓢ Supporting Information. Additional figure (PDF). This material is available free of charge via the Internet at http://pubs.acs.org.

■ AUTHOR INFORMATION

Corresponding Author
*E-mail: s-slee@kist.re.kr.

■ ACKNOWLEDGMENT

This research was kindly supported by a grant from the Seed Collaborative R&D Program funded by the Korean Research Council of Fundamental Science and Technology (KRCF), and the Fundamental R&D Program for Core Technology of Materials, funded by the Ministry of Knowledge Economy, Korea.

■ REFERENCES

(1) Bowden, N. B.; Weck, M.; Choi, I. S.; Whitesides, G. M. *Acc. Chem. Res.* **2001**, *34*, 231.
(2) Whitesides, G. M.; Boncheva, M. *Proc. Natl. Acad. Sci. U.S.A.* **2002**, *99*, 4769.
(3) Xia, Y.; Gates, B.; Yin, Y.; Liu, Y. *Adv. Mater.* **2000**, *12*, 693.
(4) Caruso, F. In *Topics in Current Chemistry II*; Antonietti, M., Ed.; Springer-Verlag: Heidelberg, Germany, 2003; Vol. 227.
(5) Oldenburg, S. J.; Averitt, R. D.; Westcott, S. L.; Halas, N. J. *Chem. Phys. Lett.* **1998**, *288*, 243.
(6) Zheng, H.; Lee, I.; Rubner, M. F.; Hammond, P. T. *Adv. Mater.* **2002**, *14*, 569.
(7) Zheng, H.; Lee, I.; Rubner, M. F.; Hammond, P. T. *Adv. Mater.* **2002**, *18*, 4505.
(8) Aizenberg, J.; Braun, P. V.; Wiltzius, P. *Phys. Rev. Lett.* **2000**, *84*, 2997.
(9) Liu, J. *Circuit World* **1993**, *19*, 4.
(10) Liu, J. *Soldering Surf. Mount Technol.* **2001**, *13*, 39.
(11) Reynhout, X. E. E.; Hoekstra, L.; Meuldijk, J.; Dringkenburg, A. A. H. *J. Polym. Sci., Part A* **2003**, *41*, 2985.
(12) Wang, P. H.; Pan, C. Y. *Colloid Polym. Sci.* **2002**, *280*, 152.
(13) Li, Y.; Moon, K.; Wong, C. P. *Science* **2005**, *308*, 1419.
(14) Li, Y.; Wong, C. P. *Mat. Sci. Eng., R* **2006**, *51*, 1.
(15) Caruso, F. *Adv. Mater.* **2001**, *13*, 11.
(16) Brown, K. R.; Natan, M. J. *Langmuir* **1998**, *14*, 726.
(17) Ji, T.; Lirtsman, V. G.; Avny, Y.; Davidov, D. *Adv. Mater.* **2001**, *13*, 1253.
(18) Kaltenpoth, G.; Himmelhaus, M.; Slansky, L.; Caruso, F.; Grunze, M. *Adv. Mater.* **2003**, *15*, 1113.
(19) Zhang, Y.; Tan, Y.-W.; Stormer, H. L.; Kim, P. *Nature* **2005**, *438*, 201.
(20) Zhang, Y.; Small, J. P.; Amori, M. E. S.; Kim, P. *Phys. Rev. Lett.* **2005**, *94*, 176803.
(21) Stankovich, S.; Dikin, D. A.; Dommett, G. H.; Kohlhaas, K. M.; Zimney, E. J.; Stach, E. A.; Piner, R. D.; Nguyen, S. T.; Ruoff, R. S. *Nature* **2006**, *442*, 282.
(22) Berger, C.; Song, Z.; Li, T.; Li, X.; Ogbazghi, A. Y.; Feng, R.; Dai, Z.; Marchenkov, A. N.; Conrad, E. H.; First, P. N.; de Heer, W. A. *J. Phys. Chem. B* **2004**, *108*, 19912.
(23) Chung, D. D. L. *J. Mater. Sci.* **2004**, *39*, 2645.

(24) Shin, H.-J. *Adv. Func. Mater.* **2009**, *19*, 1987.
(25) Tung, V. C.; Allen, M. J.; Yang, Y.; Kaner, R. B. *Nat. Nanotechnol.* **2009**, *4*, 25.
(26) Moon, I. K.; Lee, J.; Ruoff, R. S.; Lee, H. *Nat. Commun.* **2010**, *1*, 73.
(27) Steurer, P.; Wissert, R.; Thomann, R.; Muelhaupt, R. *Macromol. Rapid Commun.* **2009**, *30*, 316.
(28) Kim, H.; Macosko, C. W. *Macromolecules* **2008**, *41*, 3317.
(29) Liang, J.; Wang, Y.; Huang, Y.; Ma, Y.; Liu, Z.; Cai, J.; Zhang, C.; Gao, H.; Chen, Y. *Carbon* **2009**, *47*, 922.
(30) Liu, P.; Gong, K.; Xiao, P.; Xiao, M. J. *Mater. Chem.* **2000**, *10*, 933.
(31) Dionigi, C.; Stoliar, P.; Ruani, G.; Quiroga, S. D.; Facchini, M.; Biscarini, F. *J. Mater. Chem.* **2007**, *17*, 3681.
(32) Shi, J.; Chen, Z.; Qin, Y.; Guo, Z.-X. *J. Phys. Chem. C* **2008**, *112*, 11617.
(33) Vickery, J. L.; Patil, A. J.; Mann, S. *Adv. Mater.* **2009**, *21*, 2180.
(34) Stankovich, S.; Piner, R. D.; Chen, X.; Wu, N.; Nguyen, S. T.; Ruoff, R. S. *J. Mater. Chem.* **2006**, *16*, 155.
(35) Stankovich, S.; Dikin, D. A.; Piner, R. D.; Kohlhaas, K. M.; Kleinhammes, A.; Jia, Y.; Wu, Y.; Nguyen, S. T.; Ruoff, R. S. *Carbon* **2007**, *45*, 1558.
(36) Szabó, T.; Berkesi, O.; Forgó, P.; Josepovits, K.; Sanakis, Y.; Petridis, D.; Dékány, I. *Chem. Mater.* **2006**, *18*, 2740.
(37) Li, D.; Müller, M. B.; Gilje, S.; Kaner, R. B.; Wallace, G. G. *Nat. Nanotechnol.* **2008**, *3*, 101.
(38) Silverstein, R. M.; Bassler, G. C.; Morrill, T. C. *Spectroscopic Identification of Organic Compounds*; John Wiley and Sons: New York, 1981.
(39) Ramm, M.; Ata, M.; Gross, T.; Unger, W. *Appl Phys A: Mater.* **2000**, *70*, 387.
(40) Belin, T.; Epron, F. *Mater. Sci. Eng., B* **2005**, *119*, 105.
(41) Wang, X.; Zhi, L.; Müllen, K. *Nano Lett.* **2008**, *8*, 323.